Research Article | Vol. 27, No. 5 | 4 Mar 2019 | OPTICS EXPRESS 7307
Optics EXPRESS

Experimental electric field visualisation of multi-mode dynamics in a short cavity swept laser designed for OCT applications

T. P. BUTLER,[1,2,4,*] D. GOULDING,[1,2,3] S. SLEPNEVA,[1,2] B. O'SHAUGHNESSY,[1,2] S. P. HEGARTY,[1,2] G. HUYET,[1,2,5,6] AND B. KELLEHER[2,7]

[1] *Center for Applied Photonics and Process Analysis, Department of Physical Sciences, Cork Institute of Technology, Ireland*
[2] *Tyndall National Institute, University College Cork, Ireland*
[3] *Department of Mathematics, Cork Institute of Technology, Ireland*
[4] *Currently with the Max Planck Institute of Quantum Optics, Hans-Kopfermann-Str. 1, 85748 Garching, Germany*
[5] *Currently with the Université Côte d'Azur, CNRS, Institut de Physique de Nice, F-06560 Valbonne, France*
[6] *National Research University of Information Technologies, Mechanics and Optics, Saint Petersburg, Russia*
[7] *Department of Physics, University College Cork, Ireland*
[*] *thomas.butler@mpq.mpg.de*
www.cappa.ie

Abstract: An experimental study into the modal dynamics of a short cavity, fast frequency-swept laser is presented. This commercially available external cavity swept source is designed for use in optical coherence tomography (OCT) applications and displays a number of dynamic lasing regimes during the course of the wavelength sweep. Interferometric full electric field reconstruction is employed, allowing for measurement of the laser operation in a time-resolved, single-shot manner. Recovery of both the phase and intensity of the laser output across the entire sweep enables direct visualization of the laser instantaneous optical spectrum. The electric field reconstruction technique reveals the presence of multi-mode dynamics, including coherent mode-locked pulses. During the main part of the imaging sweep, the laser is found to operate in a second harmonic sliding frequency mode-locking regime. Examination of the modal evolution of this coherent regime reveals evidence of previously unobserved frequency switching dynamics.

1. Introduction

Swept frequency lasers are a class of laser whose output wavelength is modulated over a broad bandwidth at a high repetition rate in a continuous or quasi-continuous manner. Swept lasers are used in a variety of optical sensing techniques, including spectroscopy [1], thermometry [2], optical frequency domain reflectometry (OFDR) [3], fibre Bragg grating sensor arrays [4] and swept source optical coherence tomography (SS-OCT) [5]. OCT is a medical imaging technique used to create three-dimensional volumetric images of semi-transparent biological samples such as the eye [6] or tooth [7]. The development of swept sources has been primarily driven in the last 15 years by the introduction of Fourier domain OCT methods and the adoption of swept lasers as novel light sources [8]. Swept source and Fourier domain OCT methods have been shown to provide much higher sensitivities than conventional time domain techniques due to Fourier domain parallelization of the image noise [9–11]. Furthermore, swept frequency lasers can enable significantly higher imaging rates than previous techniques [12].

Since the demonstration of the first swept sources designed for OCT in 1997 [8], a number of laser cavity designs have been proposed for creating swept sources. In its simplest form, a

#351534 https://doi.org/10.1364/OE.27.007307
Journal © 2019 Received 14 Nov 2018; revised 30 Dec 2018; accepted 31 Dec 2018; published 27 Feb 2019

Optics EXPRESS

swept source laser is similar in design to a conventional tunable laser. Apart from a gain medium and feedback mechanism the laser requires a way to internally filter the output emission. In the ideal case, such a tunable output filter will allow the laser to change output wavelength rapidly and continuously without added noise, mode-hopping, or other dynamics. Extended cavity configurations, including grating [13] and polygonal mirror [14] reflectors, have commonly been used; as well as all-fiber Fabry-Pérot tunable cavities as found in Fourier domain mode-locked lasers (FDMLs) [15]. Recently, progress has been made toward producing shorter cavity length configurations, which can enable cheaper and more compact sources. This has lead to the development of multiple commercially available swept sources utilizing short external cavities based on micro-electro-mechanical systems (MEMS) [16, 17]. Such devices have been shown to exhibit multiple dynamic behaviors over the course of a single wavelength sweep [18]. Deeper and more complete characterization of the behavior of these sources allows for greater understanding of how the laser dynamics can affect performance in imaging and sensing applications. As such, study of the many dynamic regimes that manifest in these lasers is an important aspect of determining their suitability for novel applications, and optimizing the design of future laser sources.

Previously, characterization of swept source lasers has involved studying temporal- or sweep-averaged properties of laser devices such as the coherence roll-off [19] or instantaneous linewidth [20]. Time-resolved studies of swept sources has relied solely on intensity measurements, such as the sliding RIN [19] and direct intensity measurements [18], or theoretical studies [21]. Recently we have demonstrated an interferometric self-delayed heterodyne technique based on a 3×3 passive fiber coupler which can reconstruct the phase of broadband swept sources [22, 23]. Simultaneous measurement of both the phase and intensity of the output laser field allows for a time-resolved, single-shot measurement of the full sweep complex electric field. This knowledge enables analysis of multiple important swept source parameters, including sweep shape, spectrum, instantaneous frequency, instantaneous linewidth, and coherence roll-off. Recovery of the electric field also allows for study of fast laser dynamics. Time-resolved visualization of single-mode and mode-hopping dynamics has been performed with this technique, revealing the fundamental modal dynamics of both VCSEL and external cavity lasers [24]. In this work, the technique is used to provide for the first time direct experimental analysis of the multi-mode dynamics occurring during the fast spectral sweeping of a short cavity laser.

The device used in this work is a commercially available swept laser produced by AXSUN technologies Inc. [17]. The laser's emission is centered at 1310 nm, with a full sweep bandwidth of over 100 nm. The sweep rate of the laser is approximately 50 kHz, leading to a ~20 μs long sweep. The laser uses an external cavity consisting of a semiconductor optical amplifier (SOA) and external reflectors. One of the external reflectors is a tilted micro-Fabry-Pérot cavity [25–27]. This multi-spatial-mode cavity acts as a retro-reflecting intra-cavity spectral filter with a full-width half-maximum bandwidth of approximately 15 GHz. By constructing the cavity with a MEMS membrane structure, the central filter frequency can be rapidly tuned across a the entire gain bandwidth of the SOA. Due to the commercial nature of the device, parameter tuning was unavailable.

The laser phase is measured using a 3×3 fiber interferometer. This interferometric technique allows for the measurement of the phase difference between two input signals, and has previously been used to investigate the dynamics of externally injected semiconductor lasers [28], as well as the phase of dissipative solitons in semiconductor lasers [29]. In order to reconstruct the entire laser sweep, which spans approximately 18 THz, a delayed copy of the swept signal is used as the reference in a heterodyne field measurement. Self-referencing of the laser signal ensures that the measurement is only limited by the requirement that the instantaneous bandwidth of the signal be smaller than the electronic detection bandwidth (in this case 12 GHz). The output laser intensity is recorded simultaneously with the reconstructed phase, leading to a single-shot measurement of

Optics EXPRESS

the complex electric field. This full complex electric field shares the temporal resolution of the real-time oscilloscope used to measure the detected intensity signals (25 ps), and the duration of a single measurement is limited only by the memory depth of the oscilloscope (250 μs). For a more complete description of the phase reconstruction technique, see [22] and [23].

2. Full sweep reconstruction and intensity dynamics

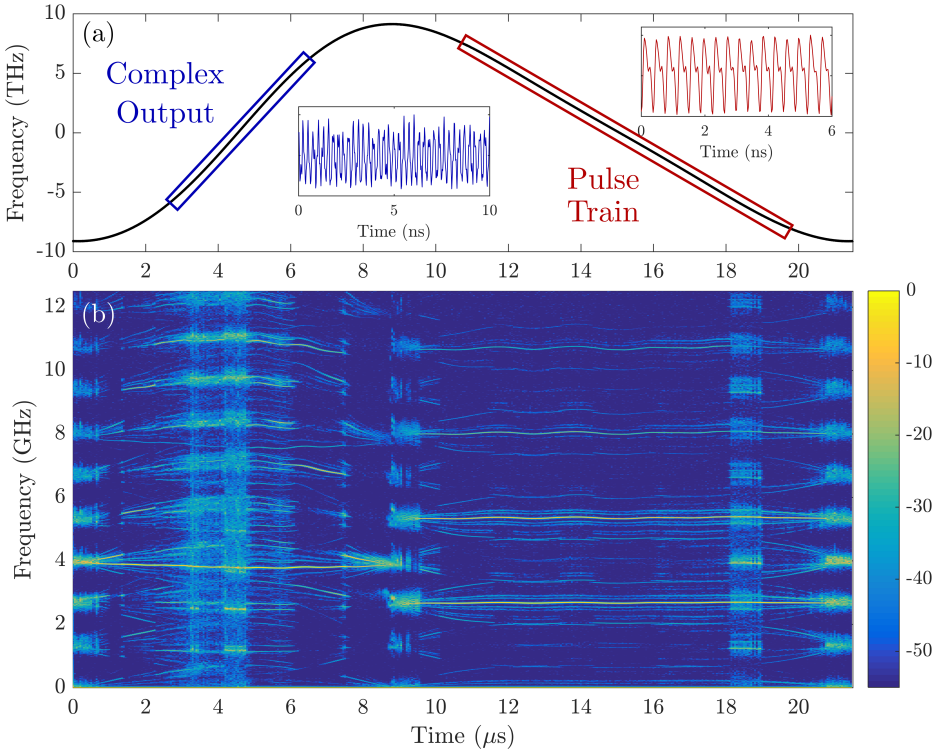

Fig. 1. (a) Instantaneous frequency of the short cavity laser during a single sweep period. The backward sweep (blue) consists of a complex output intensity, while the forward sweep (red) contains a periodic pulsed output. (b) Time-resolved electronic spectrum of the sweep intensities reveal the various dynamic regions. Intensity in dB is indicated by the color-map.

Figure 1(a) presents the instantaneous frequency, $f(t)$, of a single sweep period, calculated from the reconstructed electric field. The instantaneous frequency is reported relative to the central frequency (equivalent to 1310 nm). The sweep is asymmetric in the time domain, with the positive sweep section being shorter than the negative. In OCT applications, the negative frequency sweep is often referred to as the forward sweep, while the positive frequency sweep is known as the backward sweep (in accordance with the direction of the filter sweep in wavelength space). The trajectory of the frequency during the forward sweep is quasi-linear, with a maximum speed of -1.8 GHz/ns (10.1 nm/μs). The speed of the backward sweep is at a maximum during the center of the sweep with a value of +3.5 GHz/ns.

The time-resolved electronic spectrum of the sweep period is shown in Fig. 1(b). This spectrogram is formed by calculating the short time fast Fourier transform of the measured laser intensity. The spectrogram highlights the changing dynamics across the sweep period. At early times, during the backward sweep, the spectrum is broadband with a high noise floor. This

Optics EXPRESS

behavior is indicative of the complex output intensity, with unpredictable pulse heights and timings. The main feature of this output is a strong third harmonic frequency which dominates the repetition rate of the intensity. During the top and bottom of the laser sweep, all of the cavity harmonics can be observed. This region features mode-hopping dynamics forming in the intermediate time between the fast-moving forward and backward sweep [24].

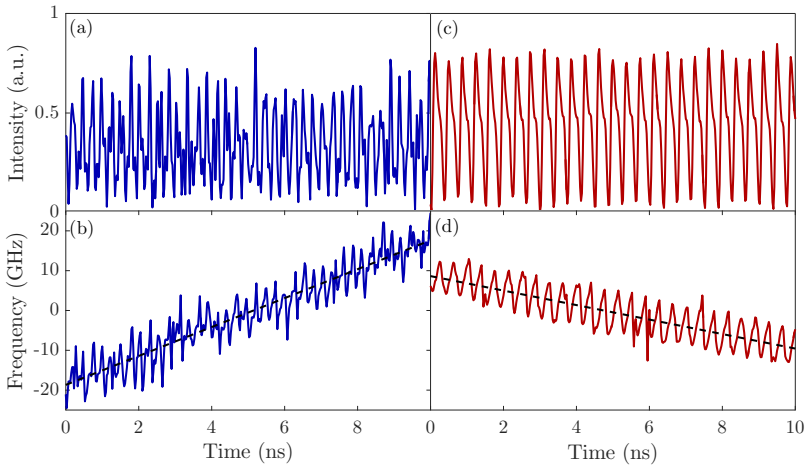

Fig. 2. (a) Experimentally measured intensity and (b) instantaneous frequency of a short section of the positive frequency sweep. (c) Intensity and (d) frequency of the mode-locking negative frequency sweep. Black lines indicate a linear fit to the frequency trajectory.

Finally, during the fast negative sweeping of the filter, the laser output exists as a series of periodic pulsations. The pulse train has a period of approximately 0.375 ns, corresponding to a repetition rate of 2.66 GHz. Coherent pulsing of swept frequency lasers has been observed previously in extended cavity configurations, and has been termed sliding frequency mode-locking (SFML) [14, 30, 31]. SFML shares many of the same traits as conventional pulsed laser mode-locking, with one major difference. As in conventional mode-locking, phase locking of the modes in the laser comb means that the modes can coherently sum to form a periodic pulse train. In the case of SFML however, each pulse is now no longer totally identical. The sweeping nature of the internal spectral filter means that each pulse now has a different and continuously changing central frequency. With a linear sweep speed of -1.8 GHz/ns and a pulse period of 0.375 ns, this implies that each of the pulses in the forward sweep will have a central frequency offset of 675 MHz.

Another important characteristic of the pulse train is revealed by the the electronic spectrum. During the negative side of the sweep, the pulse repetition frequency, frep is the second harmonic of the cavity fundamental. From the measured electronic spectrum, it is inferred that the cavity round-trip delay is twice the pulse repetition period (cavity delay of 0.75 ns or 22.5 cm roundtrip). This situation of harmonic sliding frequency mode-locking has been observed previously in other SFML devices [32], as well as very similar short cavity lasers [27, 33].

3. Multi-mode phase dynamics

Previous study of this laser system has examined the mode-hopping dynamics which occur during the slow moving region of the filter sweep [24]. In this slow-sweep regime, the switching of modes occurs as the dominant mode leaves the filter bandpass and loses gain. A new mode is then free to lase closer to the center of the filter. As the filter speed increases, however, this process becomes too slow to enable efficient lasing. Instead, the laser enters a fully multi-mode

Optics EXPRESS

regime, with the output intensity behavior depending on the direction of the sweep. It is known that this sort of sweep asymmetry is caused by the presence of the alpha factor in the SOA gain region [18].

Figure 2 presents the recovered electric field measured using the 3×3 interferometric technique. Examining the field involves considering the combination of the instantaneous intensity and frequency and is a simple way to discern the overall dynamics of the field. Figures 2(a) and 2(b) shows the experimental field measurement over a small representative section of the backward sweep, while Figs. 2(c) and 2(d) illustrates the reconstruction of a similar small section of the forward sweep. The differing phase dynamics in each case is readily apparent. While the forward sweep maintains a periodic intensity, along with a similarly structured frequency, the backward sweep dynamics are more complex and unpredictable.

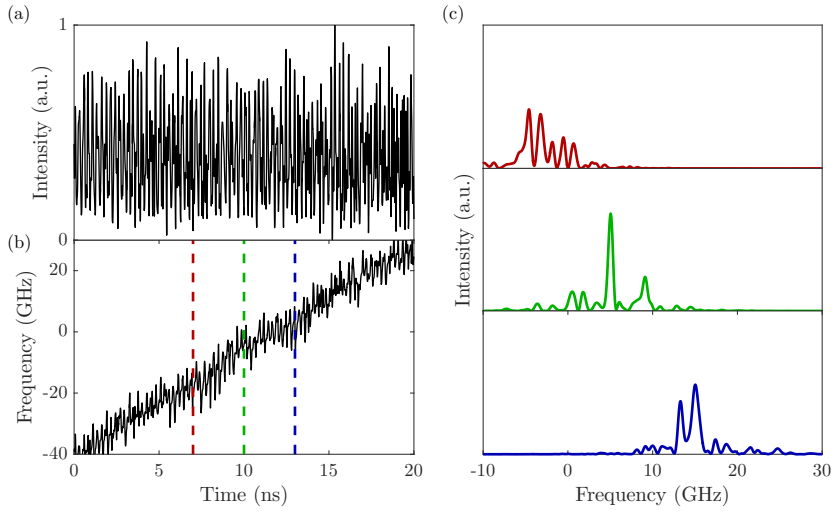

Fig. 3. (a) and (b): Recovered backward sweep electric field. (c) Instantaneous optical spectrum at three different points indicated by the dashed lines in (b). See Visualization 1 for an animation of this measurement.

The intensity dynamics observed in both the forward and backward sweep suggest that the full electric field during these regions is composed of contributions from multiple laser modes. The single-valued frequency function, $f(t)$, however, is not particularly useful for decoupling the behavior of these discrete cavity modes. A more physically intuitive view can be acquired by calculating the instantaneous optical spectrum of the field at multiple points along the electric field trajectory. The electric field signal is first windowed in the time domain using a Hamming window, before computing the absolute value squared of the Fourier transform of the resulting signal. The central position of the short time-window is then altered, resulting in a view of the laser power spectral density resolved in both the temporal and spectral domains. This procedure has been proven to be capable of resolving individual cavity modes, as well as the interactions of multiple simultaneously lasing modes [24].

An example instantaneous spectrum output is shown in Fig. 3. This figure shows the optical spectrum measured at three nearby consecutive times during the sweep. In each case, the laser spectrum is formed from multiple modes, with between 2 and 5 modes dominating the output. The center frequency of the spectrum is different at each point, as expected from the moving filter. There does not appear to be much structure present between each instantaneous spectral snapshot, with the width, intensity, and distribution of modal power seemingly uncorrelated. This modal

Optics EXPRESS

structure manifests as the complex intensity seen previously. The wide-bandwidth electronic spectrum which accompanies certain parts of the sweep (as seen in Fig. 1(b)) is reminiscent of stochastic or chaotic dynamics. Further examination of the spectral evolution is possible by once again computing the short-time Fourier transform, this time of the full complex field. The field spectrogram in Fig. 4 presents a two dimensional time-frequency picture of the instantaneous optical spectrum. Compared to the previous figure, the temporal window function is now moved across the field in 250 ps intervals, rather than just calculated at three distinct points.

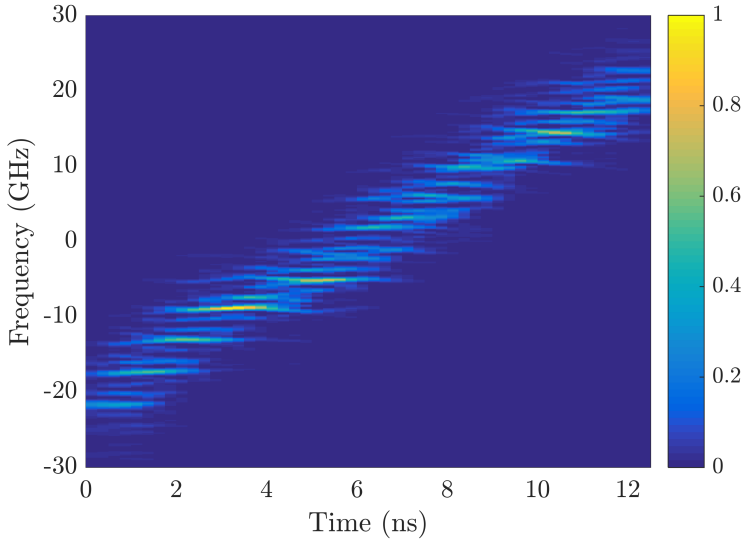

Fig. 4. Two dimensional optical spectrogram of the backward sweep. Intensity is indicated by the linear color-map.

The broader view of the modal dynamics in Fig. 4 reveals that although every mode in the spectrum is active at some point, the distribution and evolution of the modal energy does not follow a simple pattern. In contrast to the backward sweep dynamics, the modal evolution of the forward sweep is much easier to understand. The presence of periodic pulsations are a clear sign that there exists some fixed phase relationship which persists through the continuous frequency shift of the laser output. Unlike in conventional mode-locking, where a fixed phase exists between all of the lasing modes, the existence of the moving filter means that the phase relationship must survive the birth and death of multiple modes over a very short timescale. In this case, some sort of coherence transfer mechanism must exist to ensure that the phase locking of the currently active modes is passed along the modal comb and contributes to a different set of modes later in the sweep. Numerical studies of these types of swept external cavity lasers have shown that this coherence transfer can be achieved by four-wave-mixing (FWM) of the modes in the non-linear gain region [31]. If two modes mix in the SOA, they can produce a FWM idler at a new frequency, offset by the frequency difference between the two modes. This idler signal will coincide with the position of a new mode which is born as it enters the gain region beneath the filter passband. The FWM signal can then seed the lasing of the new mode, establishing a phase relationship between the previously existing modes and the newly born one. The newly seeded mode can increase in power, as it approaches the center of the filter passband and receives more gain. This allows further FWM to occur and continue to seed the sliding frequency mode-locking dynamics.

As discussed above, the SFML occurring in the short cavity laser contains two pulses per cavity round-trip. This means that only every second optical mode should be active, and the

Optics EXPRESS

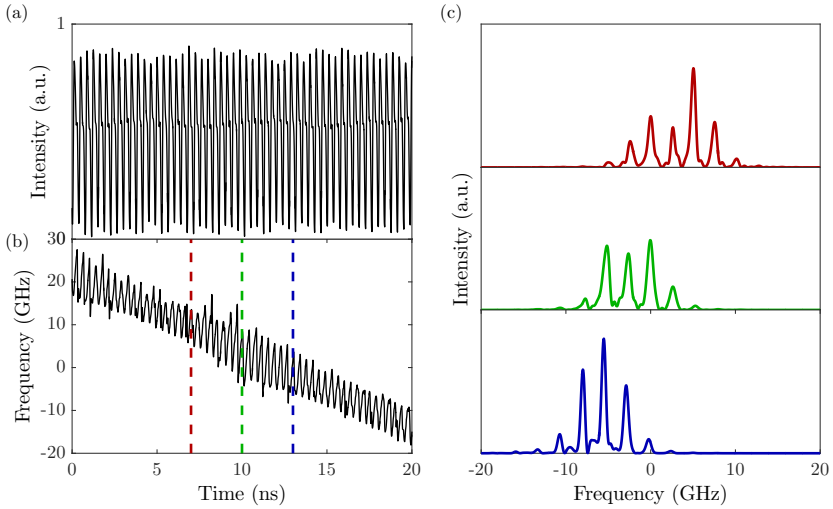

Fig. 5. (a) and (b): Recovered forward sweep electric field. (c) Instantaneous optical spectrum at three different points indicated by the dashed lines in (b). See Visualization 2 for an animation of this measurement.

FSR will be consequently twice that of the backward sweep. Figure 5 shows some snapshots of the optical spectrum during the SFML, confirming that this is indeed the case. Compared to the earlier complex dynamics, the modal distribution in the forward sweep is much more well structured. Approximately four dominant modes are observed at each point, while the envelope of the spectrum remains relatively constant. The only major difference between each of the spectra is the shift of the central frequency forced by the filter.

The full two dimensional spectrogram of the SFML is presented in Fig. 6. The evolution of the modes here is consistent with the FWM-based description of SFML described above. Beneath the filter passband, every second mode is active (due to the second-harmonic SFML), with a new mode being born approximately every 2 ns. Each mode has a lifetime of 5 to 7 ns. Overall, the shape of the spectrum remains relatively constant, with no change in the spectral width as the filter sweeps.

This visualization of the instantaneous optical spectrum of the mode-locking region further reveals an important aspect of the laser in the context of imaging. This part of the field is the sweep section most often used in optical coherence tomography applications. It has been previously shown that the instantaneous linewidth of this part of the sweep is ~5.7 GHz [22]. This value of the instantaneous linewidth is important as it can set a limit on the maximum achievable imaging depth in swept source OCT. This direct measurement of the modal evolution of the laser field now highlights that the major contributing factor affecting the linewidth is due to existence of multiple modes existing simultaneously, necessitating a spectral FWHM of 4 to 6 FSRs. Although the linewidth of each cavity mode is in the sub-GHz region, the dynamics of SFML impose a deterministic limit on the value of the instantaneous linewidth. In the context of OCT imaging, this dynamic behavior may represent a maximum achievable imaging depth. In order to improve upon this limitation, it will be necessary to achieve a single mode swept lasing regime, as seen for example in the swept source VCSEL [34].

Optics EXPRESS

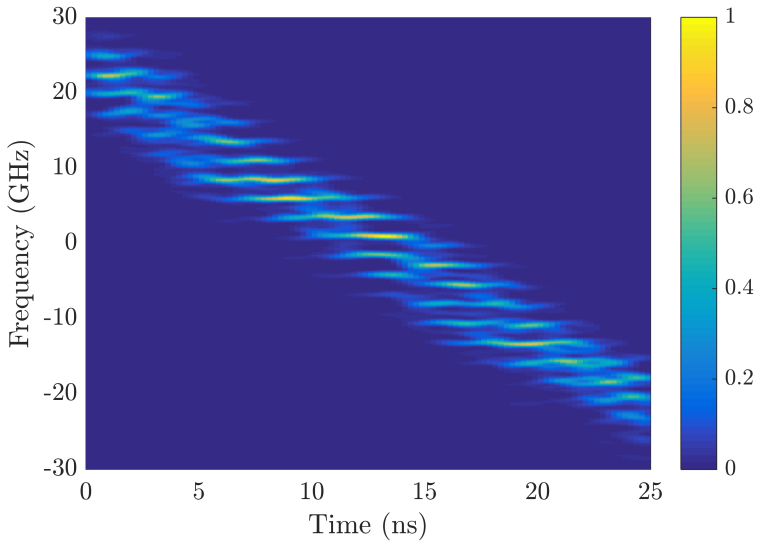

Fig. 6. Two dimensional optical spectrogram of the mode-locked pulses formed during the forward sweep, containing approximately 67 mode-locked pulses. Intensity is indicated by the linear color-map.

4. Half-FSR switching

There remains one other dynamic feature observed in the harmonic SFML regime that can be examined. This feature appears as a small shift in the frequency of the laser comb lines as the field is evolving. The slight shift can be seen in Fig. 6, at the 14-15 ns point, where there exists a dislocation in the comb mode positions. These events occur periodically throughout the SFML regime. This frequency shift of the comb can be viewed as a shift in the carrier envelope offset frequency, f_{CEO}. The CEO frequency is one of the 2 parameters that determines the frequency comb structure that is supported by the laser cavity. This description of the laser mode structure takes the form:

$$f_n = f_{\mathrm{CEO}} + n * f_0, \tag{1}$$

where f_n is the frequency of the n^{th} combline, n is an integer, and f_0 is the laser resonator free spectral range. Due to the second harmonic nature of the pulse train presented here, the laser oscillates only on either the set of even ($n = 0, 2, 4, 6, \ldots$) or odd ($n = 1, 3, 5, 7, \ldots$) modes at any given time.

Figure 7(a) shows a more clear view of the switching phenomenon. The figure presents the time-averaged spectrum of a section of the periodic pulse train. It is seen that the optical spectrum is modulated by a periodic envelope. Furthermore, each period of this over-modulation corresponds to a shift in the carrier envelope offset frequency, f_{CEO}. The switching events that occur are described by changes in the carrier envelope offset frequency equal to half of the laser FSR. It should be noted that because the laser is operating in the second harmonic region, the spacing between each mode f_{rep} is equal to twice the FSR f_0 of the cavity.

Evidence of the half-FSR switching can also be seen in the direct intensity of the laser, confirming that it is a real behavior and not an artifact of the phase reconstruction process. Figure 7(b) presents the RF electronic spectrum of a section of mode-locking. This measurement is computed from the Fourier transform of the directly measured intensity of the laser. Often in the case of a second harmonic mode-locked laser, it is expected while the main electronic beat tone will be at twice the cavity roundtrip, $2f_0$, there will also be a smaller tone at the fundamental

Optics EXPRESS

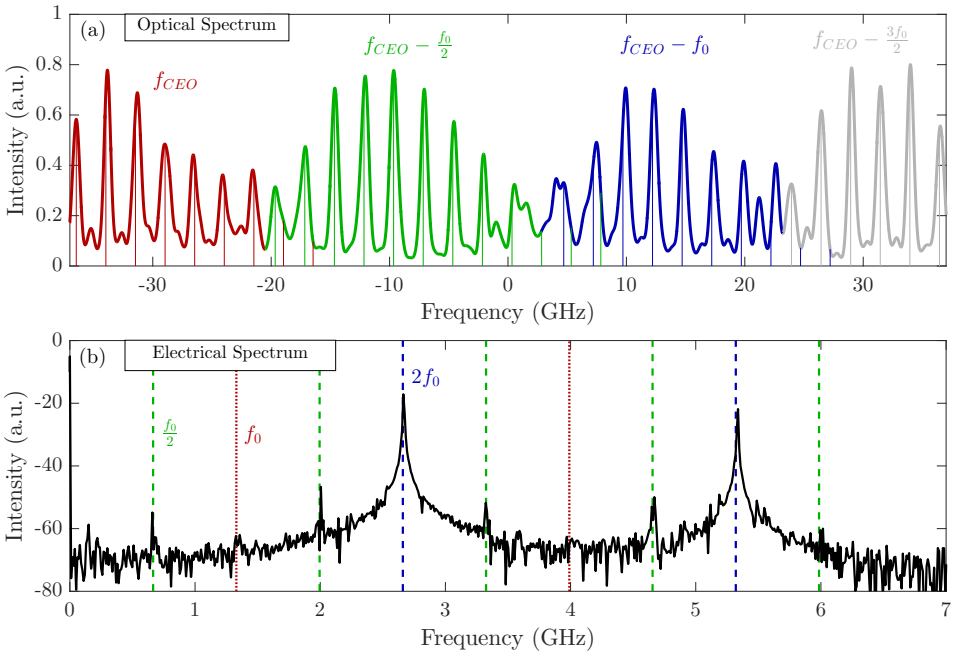

Fig. 7. (a) Section of the experimentally measured optical spectrum during the forward sweep mode-locking laser output. Each section of the spectrum has a CEO frequency offset by half of the FSR, f_0. (b) Electronic spectrum of the same mode-locked intensity.

harmonic, known as the supermode noise. The supermode noise beat term stems from the noise driven spontaneous switching of the laser between the two possible harmonic mode-locking modal states, i.e. switching from the n = even to n = odd modes. The small temporal overlap of the two states causes some modes to lase simultaneously with only one FSR separating them. When detected on a photodiode, heterodyne beating occurs strongly at $2f_0$, with some beating between comb modes separated by f_0 during the supermode switching time period.

In the short cavity laser RF spectrum, there is no supermode noise present. Each of the odd harmonics in fact are totally suppressed by over 40 dB relative to the main repetition rate tone. However, there does exist other heterodyne beat signals, located at half-integer multiples of the FSR, $0.5f_0$, $1.5f_0$, $2.5f_0$, etc. These tones suggest that whenever a switching event occurs in the laser comb, the frequency spacing between the two states occurs at a half-FSR difference, exactly as seen in the reconstructed optical spectrum of Fig. 7(a).

While the time-averaged optical and electronic spectra show the presence of a half-FSR switch, it remains to be seen why this switching occurs. The basic model of SFML does not predict any such periodic changes. Unlike in traditional supermode noise or mode-hopping, the events do not occur randomly, but at regular intervals in the sweep. This deterministic behavior implies that it has a deterministic origin. One possible origin of the switching events could be an effect of the sliding frequency intra-cavity spectral filter. Figure 8 plots the period of the switching dynamics across the entire forward sweep. The time between each switching event is seen to be highly correlated to the inverse of the current sweep speed of the filter expressed in GHz/ns. The sweep speed of the filter is determined by fitting a polynomial to the reconstructed instantaneous frequency $f(t)$ and calculating the derivative of the polynomial. This correlation of the switching period and the sweep speed means that in the frequency domain, the switching event occurs each time the filter has moved by a constant amount. This amount is equal to the proportionality

Optics EXPRESS

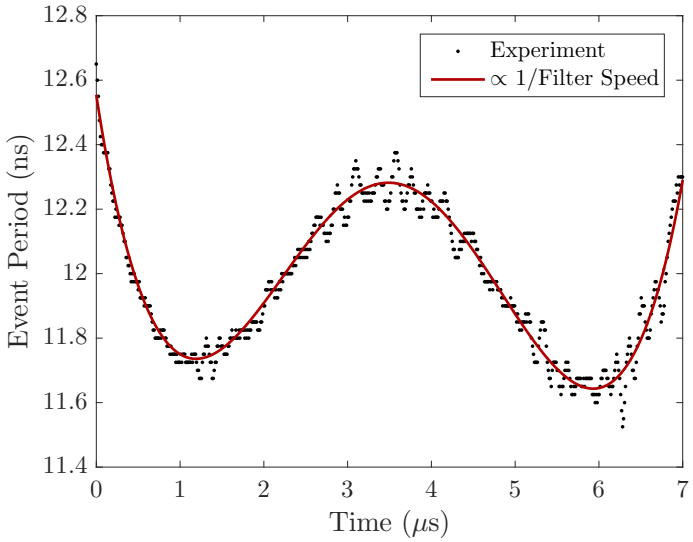

Fig. 8. Half-FSR switching period plotted over the entire forward sweep. The period is directly proportional to the filter sweep speed, shown as the solid line fit.

constant of 21.25 GHz in Fig. 8. This spectral bandwidth of a group of modes in between switching events matches the modulation envelope of the optical spectrum seen in Fig. 7(a). Because of the multi-spatial mode nature of the sweeping filter, it is believed there may be a time-varying phase imparted to the light which is back-reflected into the cavity. This phase change may be the driving force controlling the observed periodic CEO frequency hops. A similar half-FSR switching behavior has been observed in a ring cavity spectral filter [35].

5. Conclusion

This work has presented a comprehensive examination of the multi-mode dynamics present in a short cavity swept source laser. Interferometric electric field reconstruction has allowed for complex time-resolved multi-mode interactions to be observed during the fast positive and negative frequency sweep of the laser. The dynamics of the two sweep sides have been compared, with complex emission during the backward sweep and second harmonic sliding frequency mode-locking occurring during the forward sweep. It has been found that the main contribution to the device linewidth during the fast sweeping sections stems from the deterministic spectral width of the multi-mode dynamics, rather than any phase noise contribution. Calculating the instantaneous optical spectrum of the field allowed for visualization of the modal structure, lifetime, and evolution. As well as SFML, half-FSR switching was also observed for the first time in a swept source system. The real-time, single-shot measurement of the electric field allowed for characterization of this switching behavior. It has been shown to be highly correlated with the movement of the intra-cavity filter.

Funding

Science Foundation Ireland (SFI) (11/PI/1152, 12/RC/2276).

Acknowledgments

The authors would like to thank Bart Johnson of Axsun Inc. for his valuable discussion.

Optics EXPRESS

References

1. S. T. Sanders, D. W. Mattison, J. B. Jeffries, and R. K. Hanson, "Rapid temperature tuning of a 1.4 mm diode laser with application to high-pressure H_2O absorption spectroscopy," Opt. Lett. **26**(20), 1568-1570 (2001).
2. L. Kranendonk, X. An, A. Caswell, R. Herold, S. Sanders, R. Huber, J. Fujimoto, Y. Okura, and Y. Urata, "High speed engine gas thermometry by Fourier-domain mode-locked laser absorption spectroscopy," Opt. Express **15**(23), 15115-15128 (2007).
3. B. Golubovic, B. Bouma, G. Tearney, and J. Fujimoto, "Optical frequency-domain reflectometry using rapid wavelength tuning of a Cr^{4+}:forsterite laser," Opt. Lett. **22**(22), 1704-1706 (1997).
4. S. Yun, D. Richardson, and B. Kim, "Interrogation of fiber grating sensor arrays with a wavelength-swept fiber laser," Opt. Lett. **23**(11), 8438-8445 (1998).
5. F. Lexer, C. Hitzenberger, A. Fercher, and M. Kulhavy, "Wavelength-tuning interferometry of intraocular distances," Appl. Opt. **36**(25), 6548-6553 (1997).
6. I. Grulkowski, J. Liu, B. Potsaid, V. Jayaraman, C. Lu, J. Jiang, A. Cable, J. Duker, and J. Fujimoto, "Retinal, anterior segment and full eye imaging using ultrahigh speed swept source OCT with vertical-cavity surface emitting lasers," Biomed. Opt. Express **3**(11), 2733-2751 (2012).
7. K. Imai, Y. Shimada, A. Sadr, Y. Sumi, and J. Tagami, "Noninvasive cross-sectional visualization of enamel cracks by optical coherence tomography in vitro," J. Endod. **38**(9), 1269-1274 (2012).
8. S.R. Chinn, E.A. Swanson, and J.G. Fujimoto, "Optical coherence tomography using a frequency-tunable optical source," Opt. Lett. **22**(5), 340-342 (1997).
9. J.F. de Boer, B. Cense, B.H. Park, M.C. Pierce, G.J. Tearney, and B.E. Bouma, "Improved signal-to-noise ratio in spectral-domain compared with time-domain optical coherence tomography," Opt. Lett. **28**(21), 2067-2069 (2003).
10. R. Leitgeb, C. Hitzenberger, and A. Fercher, "Performance of Fourier domain vs. time domain optical coherence tomography," Opt. Express **11**(8), 889-894 (2003).
11. M. Choma, M. Sarunic, C. Yang, and J. Izatt, "Sensitivity advantage of swept source and Fourier domain optical coherence tomography," Opt. Express **11**(18), 2183-2189 (2003).
12. C. Eigenwillig, W. Wieser, B. Biedermann, and R. Huber, "Subharmonic Fourier domain mode locking," Opt. Lett. **34**(6), 725-727 (2009).
13. R. Huber, M. Wojtkowski, J. Fujimoto, J. Jiang, and A. Cable, "Three dimensional and C-mode OCT imaging with a compact, frequency swept laser source at 1300 nm," Opt. Express **13**(26), 10523-10538 (2005).
14. S. H. Yun, C. Boudoux, G. J. Tearney, and B. E. Bouma, "High-speed wavelength-swept semiconductor laser with a polygon-scanner-based wavelength filter," Opt. Lett. **28**(20), 1981-1983 (2003).
15. R. Huber, M. Wojtkowski, and J. Fujimoto, "Fourier domain mode locking (FDML): A new laser operating regime and applications for optical coherence tomography," Opt. Express **14**(8), 3225-3237 (2006).
16. S. Gloor, A. H. Bachmann, M. Epitaux, T. von Niederhausern, P. Vorreau, N. Matuschek, K. Hsu, M. Duelk, and C. Velez, "High-speed miniaturized swept sources based on resonant MEMS mirrors and diffraction gratings," Proc. SPIE **8571**, 85712X (2013).
17. M. Kuznetsov, W. Atia, B. Johnson, and D. Flanders, "Compact ultrafast reflective Fabry-Pérot tunable lasers for OCT imaging applications," Proc. SPIE, **7554**, 75541F (2010).
18. S. Slepneva, B. O'Shaughnessy, B. Kelleher, S. P. Hegarty, A. Vladimirov, H.-C. Lyu, K. Karnowski, M. Wojtkowski, and G. Huyet, "Dynamics of a short cavity swept source OCT laser," Opt. Express **22**(15), 18177 (2014).
19. B. Biedermann, W. Wieser, C. Eigenwillig, T. Klein, and R. Huber, "Dispersion, coherence and noise of Fourier domain mode locked lasers," Opt. Express **17**(12), 9947-9961 (2009).
20. B. R. Biedermann, W. Wieser, C.M. Eigenwillig, T. Klein, and R. Huber, "Direct measurement of the instantaneous linewidth of rapidly wavelength-swept lasers," Opt. Lett. **35**(22), 3733-3735 (2010).
21. E. Avrutin and L. Zhang, "Dynamics of semiconductor lasers under fast intracavity frequency sweeping," IEEE 14th International Conference on Transparent Optical Networks (ICTON), 1-4 (2012).
22. T. Butler, S. Slepneva, B. O'Shaughnessy, B. Kelleher, D. Goulding, S. P. Hegarty, H.-C. Lyu, K. Karnowski, M. Wojtkowski, and G. Huyet, "Single shot, time-resolved measurement of the coherence properties of OCT swept source lasers," Opt. Lett. **40**(10), 2277-2280 (2015).
23. D. Goulding, T. Butler, B. Kelleher, S. Slepneva, S. P. Hegarty, and G. Huyet, "Visualisation of the phase and intensity dynamics of semiconductor lasers via electric field reconstruction," in *Nonlinear Dynamics: Materials, Theory and Experiments*, M. Tlidi and M. G. Clerc eds. (Springer, 2016) pp. 3-30.
24. T.P. Butler, D. Goulding, B. Kelleher, B. O'Shaughnessy, S. Slepneva, S. P. Hegarty, and G. Huyet, "Direct experimental measurement of single mode and mode-hopping dynamics in frequency swept lasers," Opt. Express **25**(22), 27464-27474 (2017).
25. D. Flanders, M. Kuznetsov, and W. Atia, "Laser with tilted multi-spatial mode resonator tuning element," US Patent App., vol. 11/158417, 2008.
26. B. Johnson and D. Flanders, "Laser swept source with controlled modelocking for OCT medical imaging," US Patent App., vol. 12/092290, 2012.
27. B. Johnson, W. Atia, M. Kuznetsov, B.D. Goldberg, P. Whitney, and D.C. Flanders, "Coherence properties of short cavity swept lasers," Biomed. Opt. Express **8**(2), 1045-1055 (2017).
28. B. Kelleher, D. Goulding, B. Baselga Pascual, S.P. Hegarty, and G. Huyet, "Phasor plots in optical injection experiments," Eur. Phys. J. D **58**(2), 175-179 (2010).

Optics EXPRESS

29. F. Gustave, L. Columbo, G. Tissoni, M. Brambilla, F. Prati, B. Kelleher, B. Tykalewicz, and S. Barland, "Dissipative phase solitons in semiconductor lasers," Phys. Rev. Lett. **115**(4), 043902 (2015).
30. S. H. Yun, "Mode locking of a wavelength-swept laser," Opt. Lett. **30**(19), 2660-2662 (2005).
31. A. Bilenca, S. Yun, G. Tearney, and B. Bouma, "Numerical study of wavelength-swept semiconductor ring lasers: The role of refractive index nonlinearities in semiconductor optical amplifiers and implications for biomedical imaging applications," Opt. Lett. **31**(6), 760-762 (2006).
32. C.A. Alonzo and S.H. Yun, "Harmonic mode locking in a sliding-frequency fiber laser," Opt. Lett. **36**(9), 1590-1592 (2011).
33. B. Johnson, W. Atia, D. C. Flanders, M. Kuznetsov, B. D. Goldverg, N. Kemp, and P. Whitney, "SNR of swept SLEDs and swept lasers for OCT," Opt. Express **24**(10), 11174-11186 (2016).
34. I. Grulkowski, J.J. Liu, B. Potsaid, V. Jayaraman, J. Jiang, J.G. Fujimoto, and A.E. Cable, "High-precision, high-accuracy ultralong-range swept-source optical coherence tomography using vertical cavity surface emitting laser light source," Opt. Lett. **38**(5), 637-675 (2013).
35. C.T. Shih and S. Chao, "Spectral shift by half free-spectral-range for microring resonator employing the phase jump phenomenon in coupled-waveguide and application on all-microring wavelength interleaver," Opt. Express **17**(10), 7756-7770 (2009).